Anomalous Noise Behaviour in ZTE Imaging

M. Weiger[1,2], and K. P. Pruessmann[3]
[1]Bruker BioSpin AG, Faellanden, Switzerland, [2]Bruker BioSpin MRI GmbH, Ettlingen, Germany, [3]Institute for Biomedical Engineering, University and ETH Zurich, Zurich, Switzerland

Introduction MRI of short-T_2 samples is frequently performed with a 3D centre-out radial acquisition scheme and ultra-short echo time (UTE) [1]. To further improve the efficiency of the radial approach, the read gradient can be switched on before hard-pulse excitation, resulting in imaging with zero echo time (ZTE) and a faster readout [2, 3] (Fig. 1). ZTE data is slightly incomplete in the *k*-space centre due to an initial dead time Δ composed by the durations of RF pulse, send-receive switching, and digital filter build-up. The *k*-space gap can be addressed by radial acquisition oversampling and algebraic reconstruction, involving finite support extrapolation [4, 5]. However, such generalised signal processing entails deviations in noise behaviour and could lead to unusual confounds due to regional noise amplification and noise correlation in the image domain. The goal of this work was to elucidate these effects by analysing noise propagation in ZTE reconstruction.

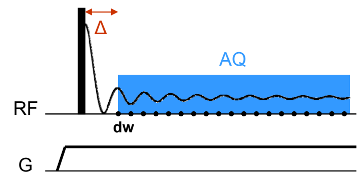

↑ **Figure 1** *ZTE acquisition scheme.*

Figure 2 *Left:* *1D noise statistics in* k*-space and image domain.* *Right:* *Correlated noise in simulated image data (real part).*

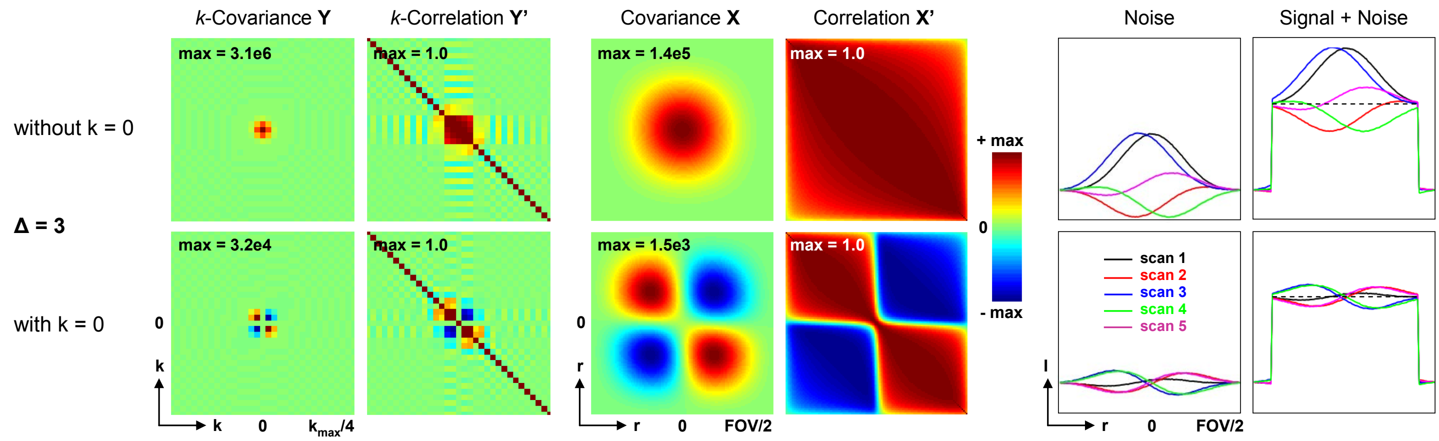

Methods The algebraic part of ZTE reconstruction provides 1D radial projection data, which are then joined by regridding to form a 3D image. In the algebraic approach [5, 6] an encoding matrix **E** is used to reflect signal encoding by gradient-driven phase modulations. Oversampling and the central gap are directly reflected by corresponding rows, or lack thereof, in the matrix **E**. Reconstruction is then achieved by the pseudoinverse $\mathbf{E}^+$. In this process, thermal noise in the input data of covariance **Ψ** propagates such as to yield image noise of covariance $\mathbf{X} = \mathbf{E}^+\mathbf{\Psi}\mathbf{E}^{+H}$. The diagonal of **X** lists the individual noise variances of the reconstructed pixels, while its off-diagonals reflect noise correlation. The latter are easier to interpret after normalisation according to $X'(i,j) = X(i,j)/(\sqrt{X(i,i)}\sqrt{X(j,j)})$, such that the resulting matrix **X'** lists correlation coefficients. When viewed in *k*-space, the same noise is of covariance $\mathbf{Y} = \boldsymbol{DFT}\,\mathbf{X}\,\boldsymbol{DFT}^H$ and the corresponding correlation **Y'**. Subsequent noise propagation into the final 3D image is governed by averaging according to the sampling density of the radial scheme, resulting in noise weighting in *k*-space proportional to k^2.

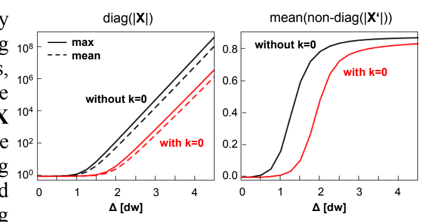

Figure 3 *Noise covariance and correlation as functions of dead time* Δ *[dwells].*

Results 1D simulations of ZTE imaging were carried out with matrix 128, oversampling 4, and Δ = 3 dwells. A sample at $k = 0$ as sometimes obtained by a measurement without gradient [7] was optionally included. Fig. 2 shows the purely real noise covariance and correlation matrices, normalised with respect to full sampling and DFT reconstruction. For better visibility, the *k*-space displays are zoomed by a factor of 4. The *k*-covariance **Y** peaks strongly in the centre reflecting noise amplification by finite-support extrapolation into the unsampled gap. Noise in this region is also strongly correlated because it derives from original data in the close neighbourhood. As a consequence, in the image domain this noise is also very strong, highly correlated, and spatially non-uniform. Including $k = 0$ considerably reduces the covariance and changes the correlation patterns (Fig. 2, second row). These calculated noise statistics are confirmed by several reconstructions of actual noise instances without and together with simulated MR signal from a 1D box (Fig. 2, right). In particular, unlike the usual grainy appearance of thermal noise, the simulations are dominated by low-frequency, shaped noise components, which reflect the predicted strong correlation. Their random nature is evident only from the fluctuation from scan to scan. As shown in Fig. 3, the observed special noise behaviour depends strongly on the dead time Δ. To confirm the theoretical findings, 3D ZTE (BW 100 kHz, matrix 128, TR 1 ms) was performed on a 7 T Bruker MRI system. The intermediate 1D noise image in Fig. 4a indeed shows the predicted behaviour. However, importantly, in the corresponding 3D reconstruction the noise is of uniform magnitude and no visible correlation. This is due to inherent averaging across the large number of 1D profiles involved, which compensates for the described noise increase in the *k*-space centre and thus eliminates highly correlated, low-frequency noise in the image domain. Only at Δ = 4.3 (Fig. 4b), further inflated noise in 1D profiles becomes strong enough to cause visible perturbations also in the final 3D data. Consistently, the ZTE image of a walnut acquired with Δ = 2.9 (Fig. 4c) is free of artefacts although the underlying 1D projections are corrupted by strong correlated noise as evident from comparison with Δ = 0.7.

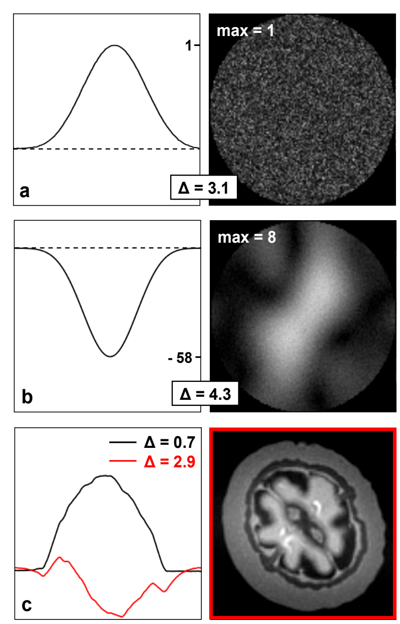

Figure 4 *Actual ZTE measurements with different* Δ*: noise (a, b), walnut (c).*

Conclusions Noise analysis of ZTE imaging has revealed peculiar and specific mechanisms of noise amplification and correlation, leading to a manifestation of noise that bears the risk of being mistaken for object structure or artefact. However, it has also been found that the strong noise averaging in the *k*-space centre inherent to 3D radial scanning compensates for this effect. Therefore, remarkably large acquisition gaps of multiple dwells are feasible, thus enabling high bandwidths, which in turn are the key prerequisite for achieving high spatial resolution in short-T_2 samples.

References [1] Glover G, JMRI 2 (1992) 47 [2] Hafner S, MRI 12 (1994) 1047 [3] Weiger M, ISMRM 2010, 695 [4] Jackson J, MRM 11 (1989) 248 [5] Kuethe DO, JMR 139 (1999) 18 [6] Pruessmann KP, NMR Biomed 19 (2006) 288 [7] Kuethe DO, MRM 57 (2007) 1058